Two-Mode Boiling on a Horizontal Heating Wire

D. J. Lee and S. M. Lu
Chemical Engineering Dept., National Taiwan University, Taipei, Taiwan, ROC

Two-mode boiling on a horizontal heated wire immersed in a pool of liquid under atmospheric pressure has been investigated. Methanol, acetone, isopropanol, and isobutanol were boiled using wires made of tungsten (0.15, 0.50, 0.82, 1.01, and 1.55 mm dia.), tantalum (0.30 and 0.82 mm dia.), molybdenum (0.125 and 1.01 mm dia.), and titanium (1.01 and 1.55 mm dia.). Two-mode boiling may be steady or unsteady. In steady two-mode boiling, both modes of boiling are stationary on the wire. The applied current in this case is referred to as the equilibrium current. In this article a method devised to calculate this current is discussed. The calculated results agreed well with the experimental results. In unsteady two-mode boiling, one of the two modes automatically takes over the other and boiling changes into a one-mode boiling. A method to calculate this transition velocity is presented. The calculated results correlated well with the experimental work.

Introduction

In pool boiling with an electrically heated horizontal wire, boiling on the wire is defined as nucleate boiling when the wire is covered entirely by nucleate boiling. Similarly, when the wire is covered entirely by film boiling, the boiling is defined as film boiling. In each case, the boiling is one-mode boiling (OMB). The boiling curve of an OMB is constructed by plotting the heat flux against the excess temperature, both quantities being the averaged quantities over the wire.

When boiling on a wire transits from one OMB to another OMB, such as from nucleate boiling to film boiling or vice versa, both modes of boiling are observed to coexist during transition. This is two-mode boiling (TMB). In TMB, the heat flux and excess temperature of a mode can be very different from those of the other. Nevertheless, averaged quantities of heat flux and excess temperature over the wire can be found. The curve that results from the plot of these averaged quantities is called the TMB curve. A TMB curve bridges the nucleate and film boiling curves. "Transition in boiling" as experienced by the wire is in fact a TMB, while the "true" transition boiling that exists between those two modes of boiling is confined to a section of the wire. True transition boiling does not exist by itself on the wire, and the fraction of the wire that is under true transition boiling is small. Thus, from the practical standpoint, the "global" transition in boiling as experienced by the wire as a whole is of more importance and interest than the true transition boiling which works to divide boiling on the wire into two modes of boiling.

The TMB curves for a given boiling system are dependent on the method of heating. Under constant current (CC) heating, the TMB curves are dependent on the magnitude of the applied current (Lu and Lee, 1991). Of these TMB curves, there is one curve on which the TMB is in steady state, while TMB on other curves are in unsteady state. In an unsteady-state two-mode boiling (UTMB), once the TMB is initiated, one boiling mode continues to advance until it takes over the entire wire and boiling becomes an OMB. For a given boiling system, this velocity of transition is dependent on the applied current. In the steady-state two-mode boiling (STMB), each of the two boiling modes occupies a certain length of the wire and remains so. Transition velocity is zero. This state of STMB, however, may be altered by a change in heat input, such as by a step increase in the applied voltage. A new stage of STMB, with each boiling mode taking up a new proportion of the wire, then results. A step-by-step increase in the applied voltage leads to a series of STMB that constitutes the STMB curve. It is through this series of STMB that one of the two boiling modes becomes the dominating mode and finally boiling becomes an OMB. Thus, the STMB curve is the locus of a series of STMB for which the magnitude of the electric current is the same. This specific electric current is referred to as the equilibrium current, I_E.

Very few data exists for equilibrium current. Zhukov et al. (1980) and Zhukov and Barelko (1983) investigated pool boiling of water with 100-μm platinum wire. Their plot shows that

equilibrium currents are about 2.7 to 3.1 Amp for different degrees of subcooling. Lu and Lee (1991) found that in saturated pool boiling of methanol under 1 atm using 0.5-mm tungsten wire, the equilibrium current is 24.3 amperes. Almost no other experimental measurements can be found in the open literature, and a method to estimate equilibrium current is nonexistent.

The velocity of transition in a UTMB has been studied by several investigators. Semeria and Martinet (1965) first treated the problem of dry spots forming on a hot wall cooled by a liquid. Van Ouwerkerk (1972) obtained a critical size of dry spot beyond which the dry area will grow and discussed the stability of nucleate and film boiling. Zhukov et al. (1980) analyzed wave propagation by film boiling over the surface of a heating element. By neglecting the true transition boiling zone, they obtained an equation for the propagation velocity of film boiling. Yamanouchi (1968) investigated the spray cooling of hot rods and obtained a velocity equation for the wet front which moves downward along the rod. Heat transfer from the dry section of the rod was neglected. Fedorov and Timchenko (1983) investigated the effects of true transition boiling zone on transition velocity and temperature distributions and reported that true transition zone can not be neglected. Timchenko et al. (1984) studied the effect of the shape of transition boiling curve on transition velocity and attained a similar conclusion.

In this article, the results of investigations for equilibrium current and transition velocity are presented. The method to calculate the equilibrium current is presented for the first time. Equilibrium currents of various pool boiling systems (systems with different boiling liquids and heating wires) under one atmospheric pressure are calculated and the results are compared with those determined by experiments. STMB curves have been constructed for different boiling systems. Equilibrium current is then used to calculate transition velocity. An analysis which is more refined than those that appear in the open literature is presented for the calculation of transition velocity. Transition boiling zone as well as the differences in heat-transfer coefficients on both sides of the zone have been taken into consideration. The analysis is performed for CC heating. However, other methods of heating can be easily adopted into this analysis. The calculated transition velocities are compared with experimental velocities of this and other works.

Experimental Studies

Saturation pool boiling has been conducted in a pool with a horizontally installed metal wire which is heated by the CC heating method. Detailed descriptions about the pool, the experimental method, the method of determination for equilibrium current, and the data acquisition system have been given elsewhere (Lu and Lee, 1991).

Different boiling liquids and heating wires have been used. The liquids used are methanol (MeOH), acetone (Ac), isopropanol (iPrOH), and isobutanol (iBuOH). For heating wires, the materials used are: 0.15, 0.50, 0.82, 1.01, and 1.55-mm-dia. tungsten (W) wires; 0.3 and 0.82-mm-dia. tantalum (Ta) wires; 0.125 and 1.01-mm-dia. molybdenum (Mo) wires; and 1.01 and 1.55-mm-dia. titanium (Ti) wires. Wire metals are of 99.99% purity. Wires 87 and 94 mm in length were used. For Ti wires, wire temperature was kept below 880°C to avoid phase transition of the metal. For Ta wire, the wire temperature was kept below 1,000°C to prevent the swelling and melting of the wire. The surface of Mo wire appears to be affected by detergent. Acetone was used for cleaning.

Table 1. Temperature Coefficients for Resistivity
$\rho_T = a_0 + a_1(T + T_{sat}) + a_2(T + T_{sat})$

Wire	$a_2 \times 10^{14}$	$a_1 \times 10^9$	$a_0 \times 10^9$	Remark
W	4.3347	0.2197	−16.401	$T<900$°C, T in K
	0	0.339	−19.8	$T>900$°C, T in K
Mo	1.5809	0.2507	49.98	T in °C
Ta	−3.536	0.4445	128.25	T in °C
Ti	−105.09	2.293	376.62	T in °C
Pt	−5.70	0.392	98.5	T in °C

A great number of data have been acquired through the data acquisition system. All steady-state boiling curves were drawn by a program installed in a PC/XT. For checking purposes, the critical heat flux (CHF) at hydrodynamic limitation was also determined. For W and Mo wires, experimental data can be reproduced easily. For Ta wires, if wire temperature is kept below 1,000°C, data can be reproduced. However, if any hot spot appears on the wire, temperature at that spot exceeds 1,000°C and this leads to burnout.

The boiling curves are determined experimentally by finding the averaged heat flux and excess temperature. The averaged heat flux of the wire is calculated by dividing the product of voltage and current by the surface area of the wire. The averaged wire temperature is calculated as follows. The current and voltage drop over the test section of a wire during boiling were measured directly. The electrical resistance is then calculated by Ohm's law. This resistance, with the diameter and length of the wire given, is used to calculate the wire resistivity ρ_T. The dependence of ρ_T on temperature is expressed by a second-order polynomial. ρ_T data from Hampel (1961), Smithells and Brandes (1976), Cubbery and Baker (1970), and Hahne and Grigull (1977) were used. The results are given in Table 1. The average temperature of a wire is then found by solving the polynomial listed in Table 1. The maximum errors in the heat flux and excess temperature were estimated to be within 2.7% and 4.4% respectively.

The velocity of transition zone in a UTMB was measured by recording the motion of the zone on a tape using NEC TI22A CCD camera, Sugawara SVA-1 vision analyzer, and a Panasonic video tape recorder. The width of transition zone was measured by using a 10 mW He-Ne laser beam to point out the boundaries of the zone. By replaying the tape, the velocity of transition zone was determined by measuring the time needed for a particular point in the zone to travel a fixed distance. Error in the velocity measurement is less than 5%.

Analyses

This section is divided into three parts. The first part is about the general situation, the second part is about the method to calculate the equilibrium current for STMB, and the third part is about the calculation of transition velocity in UTMB using the equilibrium current obtained in the second part.

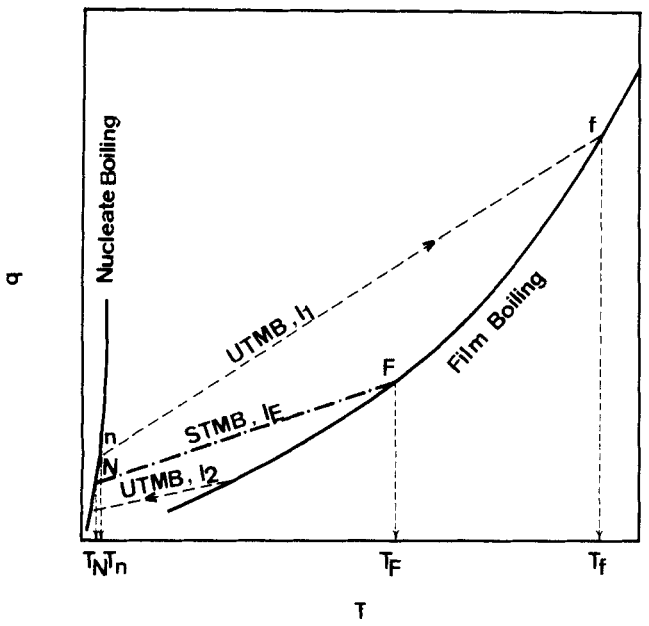

Figure 1. Nucleate, film, and two-mode boiling curves.

General

A schematic diagram of the boiling curves is shown in Figure 1. The nucleate and film boiling curves are shown by solid curves. The dot-dashed line represents the STMB curve along which the applied current is I_E. The dashed lines represent UTMB curves of given applied currents. T_n and T_f represent respectively the excess temperatures that will be assumed by the wire at the ends of a TMB curve where the OMB is either nucleate or film boiling. In Figure 2, the excess temperature along a wire in a TMB is shown. Film boiling transits to nucleate boiling within length L which, for simplicity, will be called "zone L". Over L, the excess temperature drops from T_f to T_n. The velocity of advancing or receding film boiling, u, is equivalent to the velocity of zone L. For a given heating wire, liquid, and applied current, the magnitudes of L and u in a TMB have been experimentally observed to be constant and were therefore treated as constants in this analysis. From Figures 1 and 2, we may then say that as $I \to I_E$ UTMB curve $\to$ STMB curve, and point $n \to$ point N, point $f \to$ point F, $T_n \to T_N$, $T_f \to T_F$, $L \to L_E$, and $u \to 0$. L_E is the length of transition zone in STMB.

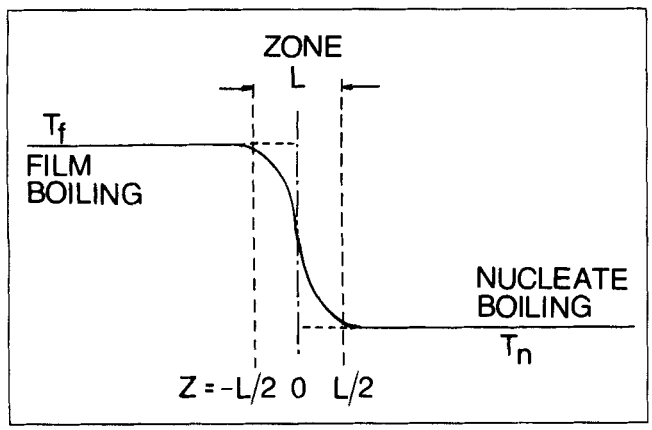

Figure 2. Temperature distribution of a wire in a two-mode boiling.

The energy equation obtained from the heat balance over a wire length dx is:

$$\rho C_p \frac{\partial T}{\partial t} = k \frac{\partial^2 T}{\partial x^2} + Q(T, I), \tag{1}$$

where

$$Q(T, I) \equiv \left(\frac{4}{D}\right)(-q_B + q), \tag{2a}$$

$$q = \frac{I^2 R}{\pi D l}, \tag{2b}$$

$$R = \frac{\rho_T l}{\pi D^2/4}, \tag{2c}$$

Equation 2a represents the difference in boiling heat transfer and heat generation. Equation 2b shows the heat generated with current I and electrical resistance R. With CC heating, I is constant. Equation 2c relates electrical resistance to electrical resistivity, ρ_T. ρ_T is related to temperature by:

$$\rho_T = a_0 + a_1(T + T_{\text{sat}}) + a_2(T + T_{\text{sat}})^2. \tag{3}$$

The coefficients in Eq. 3 are tabulated in Table 1. From Eqs. 2b, 2c, and 3, it is clear that $q = q(T, I)$ represents an UTMB curve and $q = q(T, I_E)$ represents a STMB curve. Some remark about the TMB curve should be given here. For wires with $a_2 = 0$ in Eq. 3, the TMB curves are straight lines. For many wires, this constant is rather small and therefore the TMB curves are relatively linear. Also, for wires with $a_2 = 0$, $a_1 = 0$, the TMB curves are horizontal straight lines and CC heating becomes the constant heat flux heating.

Analysis for equilibrium current

In Figure 1, the way the STMB curve is related to the two OMB (nucleate and film boiling) curves is very similar to what the "actual vapor-liquid equilibrium path" is to the two steady branches of Van der Waal's isotherm in the problem of vapor-liquid transition. For the latter, to determine the actual vapor-liquid equilibrium path, the Maxwell equal area rule has been used in spite of arguments (Pippard, 1985). This rule is expressed by the following equation:

$$\int_{v_g}^{v_l} (p - p^*)\, dv = 0 \tag{4}$$

where p is the pressure in the equation of state and p^* is the equilibrium pressure. Equation 4 represents that true transition path p is cut by actual equilibrium pressure path p^* to form two areas of equal size. Therefore, to find p^*, information about path p between the two equilibrium points which are respectively on the steady liquid and steady gas isotherms is necessary. In the vapor-liquid system, this information is provided by van der Waal's cubic equation. For many other sys-

tems, such information, however, is often not available. To overcome this difficulty, Weber (1987) investigated the "abrupt transition" that occurs with phase change in a vapor-liquid system. To find p^*, he proposed an iteration method by which the only information needed is about the two steady-state branches right near the equilibrium points. Information about the equilibrium path itself is not needed. The results of his calculation agreed well with that found by the Maxwell rule. Weber's equation is:

$$m=\frac{1}{x_g}\sum_{i=1}^{N}(p^*-idp)dv_g-\frac{1}{x_l}\sum_{i=1}^{N}(p^*+idp)dv_l \qquad (5)$$

where x_g and x_l respectively represent the quantities dv/dp (not dp/dv as shown in Weber's paper) in gas and liquid phases at points closest to the point of abrupt transition. By guessing a value for p^*, m can be calculated by Eq. 5. That particular p^* which makes $m=0$ is the equilibrium pressure that is to be found.

In the problem of pool boiling with wire, the two OMB curves (the steady nucleate and film boiling curves) represent the two steady branches between which transition may take place. Equilibrium points exist respectively on these steady branches. To find the equilibrium current for the STMB curve, an equation that corresponds to Eq. 4 can be found by the following reasoning.

For steady state boiling of any boiling mode, Eq. 1 becomes:

$$k\frac{d^2T}{dx^2}+Q(T,I)=0. \qquad (6)$$

For a STMB, "true" transition boiling occurs over $-L_E/2\le x\le L_E/2$. We may write:

$$T_{x\le -L_E/2}=T_F,\quad T_{x\ge L_E/2}=T_N \qquad (7)$$

$$\left(\frac{\partial T}{\partial x}\right)_{x\le -L_E/2}=\left(\frac{\partial T}{\partial x}\right)_{x\ge L_E/2}=0. \qquad (8)$$

Integrate Eq. 6 with respect to T from $T=T_N$ to $T=T_F$. The integration of the first term is zero because of Eq. 8. By the condition of Eq. 7 and by Eqs. 2a, 2b, and 3, the result of integration is:

$$\int_{T_N}^{T_F}(q_B-q(T,I_E))dT=0. \qquad (9)$$

Equation 9 is the equation for boiling which is comparable with Eq. 4 for the vapor-liquid system. $q(T, I_E)$ in Eq. 9 corresponds to p^* in Eq. 4. $q(T, I_E)$ represents the STMB curve which can be calculated by Eqs. 2b, 2c and 3 with $I=I_E$. Equation 9 therefore represents that the true boiling curve, q_B, is cut by the STMB curve, $q(T, I_E)$, to form two areas of equal size. There is no information available for the true transition boiling, therefore, Weber's method, which does not require such information, can be used to find I_E. The equation that corresponds to Eq. 5 is as follows:

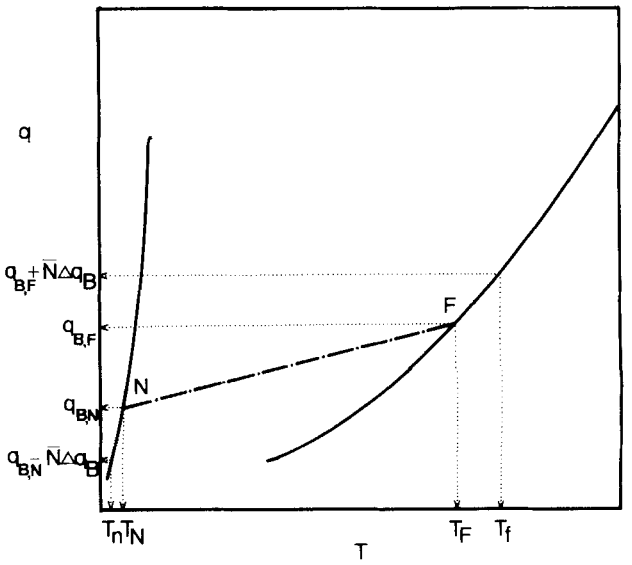

Figure 3. Quantities used in computing equilibrium current.

$$m=\left(\frac{dq_B}{dT}\right)_N\sum_{i=1}^{\bar{N}}(q_{B,N}-i\Delta q_B)(\Delta T_n)_{q_{B,N}-i\Delta q_B}-\left(\frac{dq_B}{dT}\right)_F\sum_{i=1}^{\bar{N}}(q_{B,F}+i\Delta q_B)(\Delta T_f)_{q_{B,F}+i\Delta q_B}. \qquad (10)$$

$(dq_B/dT)_N$ and $(dq_B/dT)_F$ are evaluated respectively for nucleate and film boiling at points nearest to the abrupt transition. $q_{B,N}$ and $q_{B,F}$ represent respectively the q at points N and F. Δq_B represents a small step change in boiling heat flux taken on steady nucleate or film boiling curve, and ΔT_n and ΔT_f are the corresponding temperature changes on the nucleate and film boiling curves.

To use Eq. 10, first, guess a value for I_E and obtain a guessed STMB curve q. Intersections of this guessed curve q with the nucleate and film boiling curves respectively determine the estimated N, F points and the corresponding heat fluxes, $q_{B,N}$ and $q_{B,F}$. Secondly, for a chosen value of $\bar{N}$ and for $i=1, 2, 3, \ldots, \bar{N}$, calculate $(q_{B,N}-i\Delta q_B)$ and $(\Delta T_n)_{q_{B,N}-i\Delta q_B}$ along the nucleate boiling curve. Similarly, calculate $(q_{B,F}+i\Delta q_B)$ and $(\Delta T_f)_{q_{B,F}+i\Delta q_B}$ along the film boiling curve. Figure 3 shows the situation. These values are then substituted in Eq. 10 to find m. If $m=0$, the estimate is correct and I_E is found. If not, a new I_E is estimated and the process is repeated.

Equations of nucleate and film boiling curves that are needed in the above calculation are tabulated in Tables 2 and 3. These are regression equations obtained from experimental data. For film boiling, the curves are shown in Figure 4. The experimental results agree with the equations of Breen and Westwater (1962) when heat fluxes are low. Deviation, however, is obvious when heat fluxes are high. Physical properties of the liquids used are evaluated by the property equations given by Lin (1986).

Direct use of Eq. 10, however, has proved to be numerically undesirable. The reason may be that summations of small quantities that appear in Eq. 10 may not be calculated accu-

Table 2. Equations for Nucleate Boiling

Equation	Source
$q=0.987T^4$	This Work
$q=726.4T^{2.27}$	Zhukov and Barelko (1983)

rately from the regression equations. This difficulty was overcome by using the following modification.

First, choose a value for I. Then find the respective intersection points of this TMB curve with the nucleate and film boiling curves, say points n and f, and their excess temperatures T_n and T_f. Regression equations listed in Tables 2 and 3 may be used. This process is repeated for several values of I. Secondly, for a chosen value of Δq_B, calculate $\Delta\log T_n$ and $\Delta\log T_f$ respectively at T_n and T_f. Then plot $\Delta\log T_f/\Delta\log T_n$ against $I/I_{E,\exp}$ to obtain Figure 5. This figure shows that for the wide ranges of diameters used, the magnitude of ordinate is around 1 at $I=I_E$. Therefore, the following approximation:

$$\left(\frac{dT}{T}\right)_{T_N}=\left(\frac{dT}{T}\right)_{T_F} \tag{11}$$

may be used for the regions near N and F. Equation 10 is then written as:

$$m'=\left(\frac{dq_B}{dT}\right)_N\sum_{i=1}^{\bar{N}}(q_{B,N}-i\Delta q_B)(T_n)_{q_{B,N}-i\Delta q_B}$$

$$-\left(\frac{dq_B}{dT}\right)_F\sum_{i=1}^{\bar{N}}(q_{B,F}+i\Delta q_B)(T_f)_{q_{B,F}+i\Delta q_B}. \tag{12}$$

If an estimated I makes m' zero, this I is equal to I_E. Thus, the equilibrium current can be found by trial and error.

Analysis for transition velocity

The velocity of transition zone in UTMB, u, may be found

Table 3. Coefficients for Film Boiling Equation
$q_f=C_0+C_1T+C_2T^2+C_3T^3$

d(mm)	$C_3\times10^3$	$-C_2$	$C_1\times10^{-3}$	$-C_0\times10^{-3}$	Reference
0.125	2.167	0.843	1.407	162.7	
0.15	6.087	9.615	6.815	975.6	
0.30	1.943	2.318	2.158	183.0	Methanol
0.51	0.907	0.757	0.922	74.1	
0.82	0.555	0.262	0.483	46.2	
1.01	0.882	0.905	0.830	116.1	
1.55	2.054	3.483	2.579	506.2	
0.51	0.882	1.036	1.177	126.6	Acetone
1.55	2.054	3.483	2.579	506.2	
0.51	−0.555	−1.928	−0.337	−112.5	isoPrOH
0.51	−0.0023	−0.457	0.713	126.5	isoBuOH
0.10	9.17	17.82	13.90	2,900	Zhukov and Barelko (1983), Pt Wire in Water

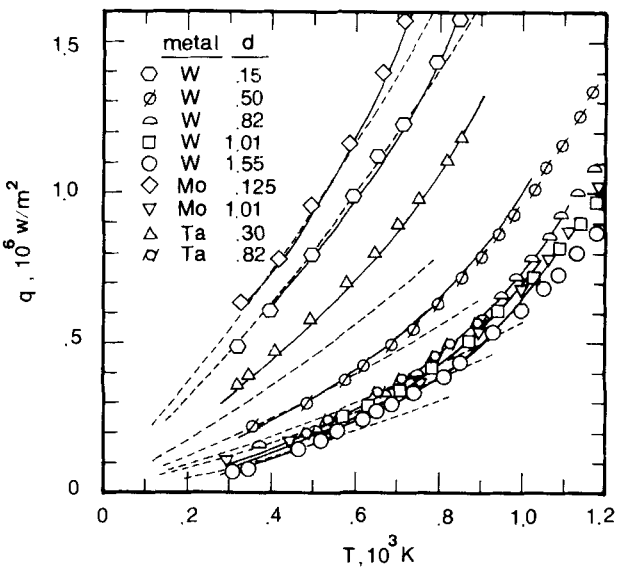

Figure 4. Film boiling curves in methanol with wires.
- - - Breen and Westwater equation (1962).
—— Regression equations given in Table 3.

by the following analysis. Equation 1 is transformed by using $z=x-ut$ and the result is:

$$\frac{d^2T}{dz^2}+\frac{u}{\alpha}\frac{dT}{dz}+\frac{1}{k}Q(T,I)=0. \tag{13}$$

The special case, $u=0$, corresponds to the case of STMB and the above equation reduces to Eq. 6.

The transition boiling curve in zone L, reasoning from its connections to the nucleate and film boiling curves, can be assumed to be a cubic polynomial of the following form:

$$q_B(T)=A_3T^3+A_2T^2+A_1T+A_0. \tag{14}$$

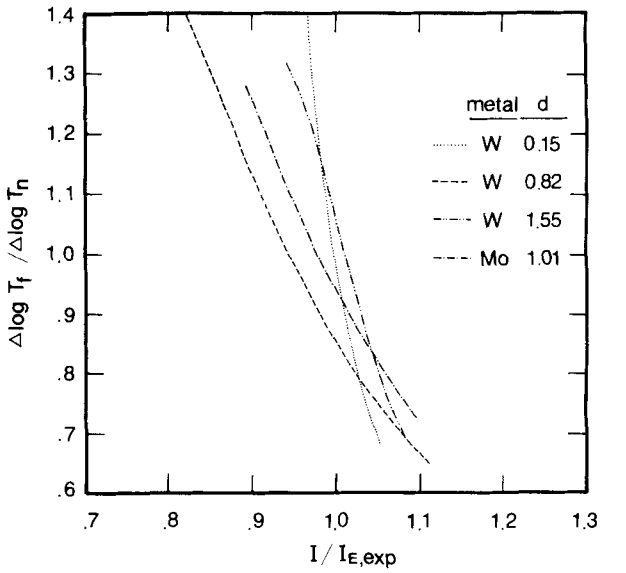

Figure 5. $\Delta\log T_f/\Delta\log T_n$ vs. I/I_E, exp.
Δq_B = 100, N = 1.

Substitute Eqs. 14, 3, 2a, 2b, and 2c into Eq. 13 and integrate the resulting equation with respect to temperature. The result is:

$$\frac{1}{2}\left(\frac{dT}{dz}\right)^2+\frac{u}{\alpha}\int\frac{dT}{dz}\,dT= -\left(\frac{N_3}{4}T^4+\frac{N_2}{3}T^3+\frac{N_1}{2}T^2+N_0T\right)+C \quad (15)$$

where C is an integration constant and:

$$N_3=\frac{-4A_3}{Dk}, \quad (16a)$$

$$N_2=\frac{-4A_2}{Dk}+\frac{16I^2}{\pi^2D^4k}a_2, \quad (16b)$$

$$N_1=\frac{-4A_1}{Dk}+\frac{16I^2}{\pi^2D^4k}(2a_2T_{\text{sat}}+a_1), \quad (16c)$$

$$N_0=\frac{-4A_0}{Dk}+\frac{16I^2}{\pi^2D^4k}(a_2T_{\text{sat}}^2+a_1T_{\text{sat}}+a_0). \quad (16d)$$

Let the temperature gradient in Eq. 15 be represented by the following polynomial:

$$\frac{dT}{dz}=\sum_{i=0}^{4}b_iT^{i/2} \quad (17)$$

which on integration results in:

$$\int\frac{dT}{dz}\,dT=\sum_{i=0}^{4}\frac{2b_i}{i+2}T^{(1+i/2)}. \quad (18)$$

Substitute the above two equations into Eq. 15 and represent the right hand side of Eq. 15 by $V(T)$. The result is:

$$\frac{1}{2}\left[\sum_{i=0}^{4}b_iT^{i/2}\right]^2+\frac{u}{\alpha}\left[\sum_{i=0}^{4}\frac{2b_i}{i+2}T^{(1+i/2)}\right]=V(T). \quad (19)$$

Comparison of the coefficients of T of the same power on both sides of the above equation gives:

$$b_{2i+1}=0, \quad i=0,\ 1 \quad (20)$$

$$b_4=\sqrt{-\frac{N_3}{2}}=\sqrt{\frac{2A_3}{Dk}}. \quad (21)$$

Substitute the above equations into Eq. 17 and obtain:

$$\frac{dT}{dz}=b_4T^2+b_2T+b_0. \quad (22)$$

Integrate the above equation as follows:

$$\int_{T_0}^{T}\frac{dT}{b_4T^2+b_2T+b_0}=\int_{z_0}^{z}dz. \quad (23)$$

The quadratic denominator on the left hand side may be written into the following product form:

$$T^2+\frac{b_2}{b_4}T+\frac{b_0}{b_4}=(T-T_f)(T-T_n). \quad (24)$$

Comparison of the coefficients of T on both sides of Eq. 24 shows that:

$$\frac{b_2}{b_4}=-(T_f+T_n) \quad (25a)$$

$$\frac{b_0}{b_4}=T_fT_n. \quad (25b)$$

Substitute Eq. 24 into Eq. 23 and carry out the integration. Assuming that the temperature profile in zone L is such that the following conditions exist:

$$z=0; \quad T=T_0, \quad (26a)$$

$$T_0=\frac{1}{2}(T_f+T_n), \quad (26b)$$

then the following solution:

$$T-T_n=\frac{(T_f-T_n)}{1+\exp(\beta z)} \quad (27)$$

where

$$\beta=b_4(T_f-T_n)=\sqrt{\frac{2A_3}{Dk}}(T_f-T_n) \quad (28)$$

is obtained. This temperature solution shows that as $|z|\to\infty$; $T\to T_f$, $T\to T_n$, showing that Eq. 7 is only approximately satisfied. This is acceptable as zone length L is usually a fraction of the test length of a wire and the wire length may be taken as of infinite length. Equations 27 and 28 further show that of the four coefficients in Eq. 14, only A_3 needs to be found.

The method for finding constant A_3 is as follows. First, define the zone length L as:

$$L=\frac{T_n-T_f}{(dT/dz)_{z=0}} \quad (29)$$

The temperature gradient in the above equation may be obtained from the differentiation of Eq. 27, that is:

$$(dT/dz)_{z=0}=-(T_f-T_n)\beta/4. \quad (30)$$

Substitute Eq. 30 into Eq. 29 and obtain:

$$L=\frac{4}{\beta}=\frac{\phi}{T_f-T_n}\sqrt{\frac{Dk}{A_3}} \quad (31)$$

where it is found that $\phi = 2.83$. Under the definition of Eq. 29, the dimensionless temperature $(T-T_n)/(T_f-T_n)$ at

$z = -L/2, L/2$ are found to be 0.8808 and 0.1192 respectively. The definition of L can be other than that given by Eq. 29. If so, the magnitudes of ϕ and $(T-T_n)/(T_f-T_n)$ will be accordingly changed.

Equation 31 can be used to evaluate the constant A_3 if L, T_f, T_n and D, k are available. As A_3 is a constant, it may be determined either from STMB or UTMB. As the measurement of L_E in STMB can be done more dependably than L in UTMB, L_E, and correspondingly I_E, T_N, T_F, were used in places of L, I, T_n, T_f in Eq. 31. T_N and T_F are found once points N and F, as shown in Figure 1, are located. Points N and F are the respective intersection points of the STMB curve with the nucleate and film boiling curves. Equations for the nucleate and film boiling are tabulated in Tables 2 and 3. The magnitudes of I_E are found by the method described in the second part of the analyses. A computer program has been written for finding T_N and T_F. Thus, by Eq. 31, constant A_3 can be determined.

To find transition velocity u, Eq. 1, with Eqs. 2a to 2c, was integrated with respect to x from $x=-L/2$ to $L/2$. The result is:

$$\frac{\pi D^2}{4} L\rho C_p \frac{d\bar{T}}{dt} = \frac{4I^2}{\pi D^2} \int_{-L/2}^{L/2} \rho_T dx - \pi D \int_{-L/2}^{L/2} q_B dx \quad (32)$$

where $\bar{T}$ is the average wire temperature over L. Outside zone L, conduction is negligible as the temperature gradient along the wire is zero, hence, heat generation is always equivalent to the heat lost by boiling. Inside zone L, if the magnitude of current L is such that heat generated is greater than heat lost by boiling, film boiling advances and zone L moves forward; if less, film boiling recedes and zone L moves backward; and if equal, zone L is stationary and the TMB is a STMB. For a STMB, Eq. 32 becomes:

$$\frac{4I_E^2}{\pi D^2} \int_{-L_E/2}^{L_E/2} \rho_T dx = \pi D \int_{-L_E/2}^{L_E/2} q_B dx \quad (33)$$

Substitute Eq. 3 respectively into Eqs. 32 and 33 and make use of the following averaged quantities:

$$\bar{T} = \frac{1}{L} \int_{-L/2}^{L/2} T dz = \frac{1}{2}(T_n + T_f) + T_{sat}, \quad (34a)$$

$$\bar{T}_E = \frac{1}{L_E} \int_{-L_E/2}^{L_E/2} T_E dz = \frac{1}{2}(T_F + T_N) + T_{sat}, \quad (34b)$$

$$\bar{q}_B \frac{1}{L} = \int_{-L/2}^{L/2} q_B dz, \quad (34c)$$

$$\bar{q}_{B,E} = \frac{1}{L_E} \int_{-L_E/2}^{L_E/2} q_{B,E} dz. \quad (34d)$$

The resulting equations are:

$$\frac{\pi D^2}{4} \rho C_p \frac{d\bar{T}}{dt} = \frac{4I^2}{\pi D^2} G(T_f, T_n) - \pi D \bar{q}_B, \quad (35a)$$

$$0 = \frac{4I_E^2}{\pi D^2} G(T_F, T_N) - \pi D \bar{q}_{B,E}, \quad (35b)$$

where

$$G(T_1, T_2) = a_2[(T_1 + T_{sat})^2 + (T_1 + T_{sat})(T_2 - T_1) + 0.3096(T_2 - T_1)^2] + a_1 \bar{\bar{T}}(T_1, T_2) + a_0. \quad (36)$$

Subtract Eq. 35b from Eq. 35a and obtain:

$$\frac{D}{4} \rho C_p \frac{d\bar{T}}{dt} = N_G - N_B, \quad (37)$$

where

$$N_G = \frac{4}{\pi^2 D^3}(G(T_f, T_n) I^2 - G(T_F, T_N) I_E^2) \quad (38a)$$

$$N_B = \bar{q}_B - \bar{q}_{B,E}. \quad (38b)$$

The derivative $d\bar{T}/dt$ in Eq. 37 can now be related to transition velocity. As zone L advances $2L$ distance, the average temperature of the first L is raised from T_n to T_f. Therefore:

$$\frac{d\bar{T}}{dt} = \frac{u(T_f - T_n)}{2L}. \quad (39)$$

Substitute the above equation into Eq. 37 and using Eq. 31, one finds that transition velocity is:

$$u = \frac{8\phi}{(T_f - T_n)^2} \sqrt{\frac{k/\rho^2 C_p^2}{DA_3}} (N_G - N_B), \quad (40)$$

where N_G is defined by Eq. 38*a* and can be calculated by using Eq. 36, and N_B can be evaluated by using the experimental data and the method described in the following section. When a TMB is a STMB, then $N_G = N_B$, and $u = 0$.

The method to calculate the boiling heat loss, N_B, is as follows. For STMB, Eq. 9 shows that:

$$\int_{T_N}^{T_F} Q(T, I_E) dT = \int_{T_N}^{T_F} (q_B - q) dT = 0 \quad (41)$$

and the STMB curve cuts the nucleate and film boiling curves in such a way that, as shown in Figure 6a, area A = area B. Thus,

$$\bar{q}_{B,E} = \frac{1}{2}(q_{B,F} + q_{B,N}) \quad (42)$$

In UTMB, the UTMB curve cuts the nucleate and film boiling curves in such a way that area A $\neq$ area B, as shown by Figure 6b. As the nucleate boiling curve is much steeper than the film boiling curve, the following approximate equation is written:

$$\int_{T_n}^{T_f} q_B dT \doteq \int_{T_N}^{T_f} q_B dT = \int_{T_N}^{T_F} q_B dT + \int_{T_F}^{T_f} q_B dT = (T_F - T_N)\bar{q}_{B,E} + \int_{T_F}^{T_f} q_B dT. \quad (43)$$

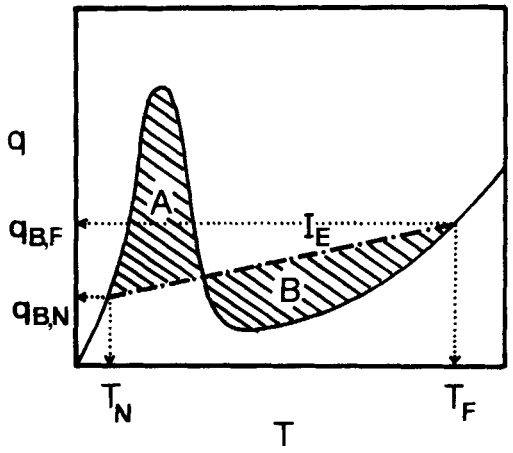

Figure 6a. $I = I_E$: area A = area B.

Divide this equation by $T_f - T_n$ and subtract from both sides the quantity $\bar{q}_B$. The resulting equation, after recalling Eq. 42, is as follows:

$$\bar{q}_B - \bar{q}_{B,E} = \left(\frac{T_F - T_N}{T_f - T_n} - 1\right)\frac{(q_{B,N} + q_{B,F})}{2} + \frac{1}{T_f - T_n}\int_{T_F}^{T_f} q_B dT. \quad (44)$$

This is the quantity of N_B in Eq. 38b. The velocity is then calculated by Eq. 40.

Results and Discussion

Equilibrium current

An example of the results of a computation is shown in Figure 7 for a boiling system using 0.82-mm-dia. W wire and methanol. Equilibrium current was found by using only a limited number of nucleate and film boiling data that are sufficiently close to the equilibrium that is yet to be found.

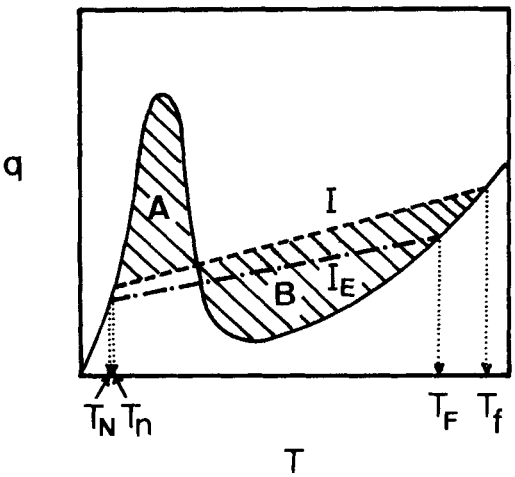

Figure 6b. $I \neq I_E$: area A $\neq$ area B.

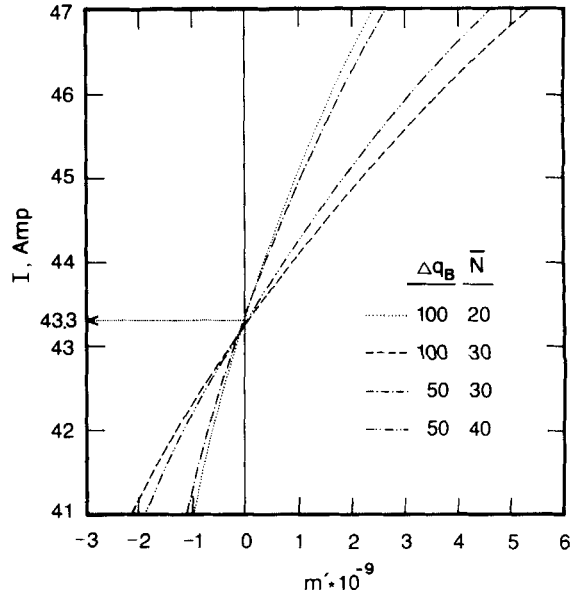

Figure 7. Example calculation: methanol, 0.82 mm tungsten wire.

The magnitudes of Δq_B and $\bar{N}$ for this example are also indicated. It is shown that $I = 43.3$ Amp makes $m' = 0$. Thus, $I_E = 43.3$ Amp for this case.

Table 4 shows the calculated and the experimental equilibrium currents for different boiling systems. Good agreement is obtained between the calculation and experiment. The last row in Table 4 shows the data from Zhukov and Barelko's (1983, 1980) for 100-μm Pt wire in water. The equilibrium current obtained by present calculation is in good agreement with their experimental data.

The STMB curves for various boiling systems are calculated from the equilibrium currents. The results are shown by the

Table 4. Calculated and Experimental Equilibrium Currents

Wire	Liquid	D (mm)	$I_{E,exp}$ (Amp)	$I_{E,cal}$ (Amp)
W	Methanol	0.15	6.0	6.4
W	Methanol	0.51	24.3*	26.1
W	Methanol	0.82	45.0	43.3
W	Methanol	1.01	55.8	55.5
W	Methanol	1.55	106.0	105.6
W	Acetone	0.51	24.6	25.7
W	Acetone	1.55	98.6	101.7
W	isoPrOH	0.51	26.2	26.7
W	isoPrOH	1.55	98.0	97.4
W	isoBuOH	0.51	25.7	25.1
W	isoBuOH	1.55	100.8	99.7
Mo	Methanol	0.125	4.7	4.4
Mo	Methanol	1.01	56.7	56.6
Ta	Methanol	0.30	11.0	12.1
Ta	Methanol	0.82	36.5	35.6
Ti	Methanol	1.01	25.2	23.3
Ti	Methanol	1.55	43.2	43.3
Pt	Water	0.10	2.75**	2.69
			2.63 †	

* From Lu and Lee (1991)
** Zhukov et al. (1980)
† Zhukov and Barelko (1983)

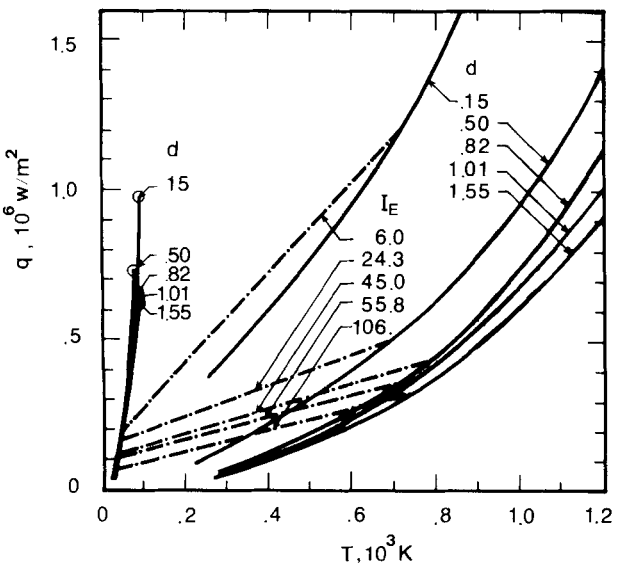

Figure 8a. Steady-state boiling curves and equilibrium currents.

Methanol: tungsten wires of diameters d mm. o for CHF; — for nucleate or film boiling; and - · - for steady two-mode boiling.

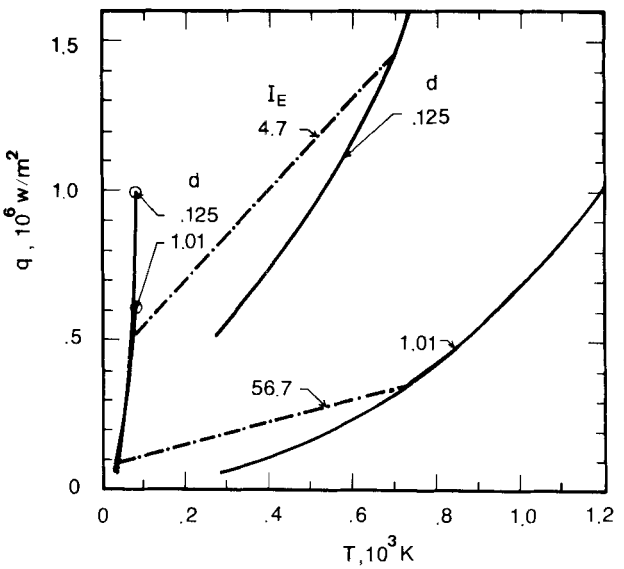

Figure 8c. Steady-state boiling curves and equilibrium currents.

Methanol: molybdenum wires of diameters d mm. o for CHF; —for nucleate or film boiling; and - · - for steady two-mode boiling.

dot-dashed lines in Figures 8a to 8c for atmospheric boiling of methanol using wires made of W, Ta, and Mo. Nucleate and Film boiling curves are represented by solid curves. For each pair of nucleate and film boiling curves, there is an unique STMB curve. These three boiling curves construct a complete steady-state boiling curve diagram. The circles at the ends of nucleate boiling curves are the critical heat fluxes which checked well with the known CHF data and were given here to make the nucleate boiling curves complete. Comparison of these figures shows that as wire diameter increases, the STMB and film boiling curves shift toward the abscissa. The degree of shift, however, decreases with increasing diameter. Figure 8a shows about 18 times increase in the current. Figures 8a and 8c show that W and Mo wires of the same diameter have about the same I_E, while Figures 8a and 8b show that for the same wire diameter, W wire has greater I_E than Ta wires.

The effects of different liquid on equilibrium current are studied by boiling methanol, acetone, isopropanol, and isobutanol respectively using W wires. Table 4 shows that for these liquids, the effects are very small. This result is expected as the effects of these liquids on nucleate and film boiling curves are small.

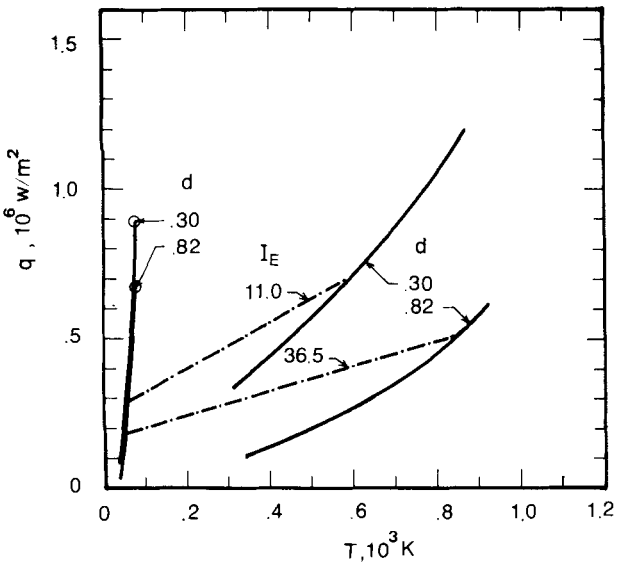

Figure 8b. Steady-state boiling curves and equilibrium currents.

Methanol: tantalum wires of diameters d mm. o for CHF; — for nucleate or film boiling; and - · - for steady two-mode boiling.

Constant A_3

Constant A_3 was calculated using zone length L_E. In the measurement of L_E, the boundaries of L_E have to be pointed out. The boundary on the nucleate boiling side can be pinned down by a laser beam which responds differently depending on whether there is a vapor film on the wire surface. This method, however, does not work on the boundary on the film boiling side. For a wire of small diameter, this boundary can still be discerned without difficulty. For a wire of large diameter, as evidenced by the change in the color of the wire, temperature at the upper surface of the wire is greater than that at the bottom surface. Therefore, uncertainty in boundary exists. This error, however, is decreased to a degree as L_E is also long in this case. Photographs taken in the experiments further suggest that temperature profile across the zone may be somewhat skewed. At present, these problems have been left untouched. Therefore, experiments do not comply exactly to the definition of L given by Eq. 29. For a given wire and a liquid, experiments show that as I increases, L decreases. This result is consistent with Eq. 31 as $T_f - T_n$ does increase with increasing I. Equation 31 also shows that the greater the

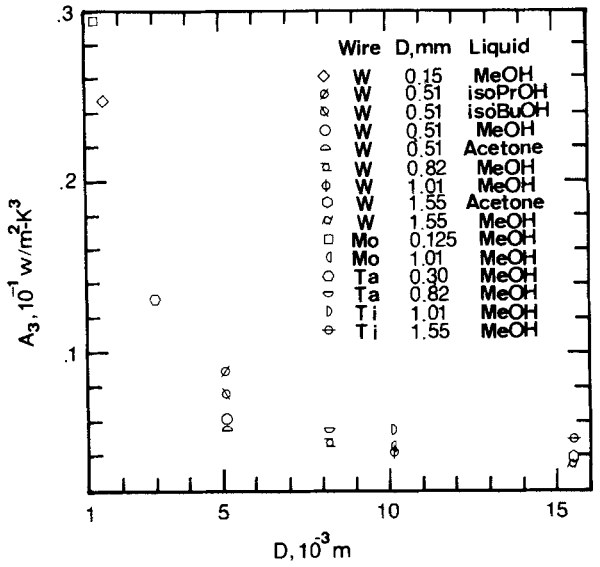

Figure 9. Constant A_3 vs. wire diameter.

wire diameter, and also the thermal conductivity, the greater the length L. It should be pointed out here that measurement of L becomes more difficult as a UTMB gets further away from the STMB. This is because that zone L moves faster and that the wire becomes either too bright (high I) or too dark (low I) and zone L becomes harder to be distinguished from the rest of the wire. Therefore, L_E was measured and used in the calculation of A_3 by Eq. 31.

Figure 9 shows the plot of A_3 against wire diameter. To correlate A_3, the following equation is proposed:

$$\frac{A_3}{A_{3,\infty}} = 0.31513 + 0.097472\,\frac{\lambda_c}{D} \tag{45}$$

where

$$\lambda_c = 2\pi\sqrt{\frac{\sigma}{g(\rho_l - \rho_v)}} \tag{46}$$

$$A_{3,\infty} = 0.00357 \tag{47}$$

Table 5. Physical Properties of Wires and Liquids

Wire	k (W/m·K)	ρ (kg/m^3)	C_p (J/kg·K)
W	121	19,300	142
Mo	121	10,200	285
Pt	70	21,450	147
Liquid	ρ_l (kg/m^3)	ρ_v (kg/m^3)	σ (N/m)
Methanol	751.1	1.222	0.0189
Acetone	790.0	2.151	0.0212
isoPrOH	718.0	2.143	0.0167
isoBuOH	730.0	2.640	0.0156
Water	958.4	0.598	0.0588

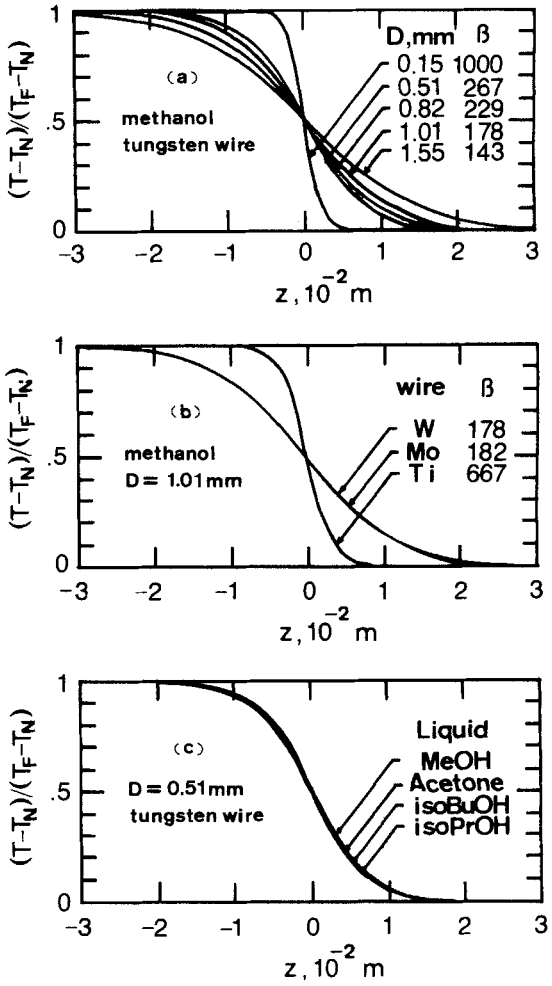

Figure 10. Wire temperature profiles.

a. Effect of diameter.
b. Effect of wire material.
c. Effect of liquid.

λ_c is the critical wave length and $A_{3,\infty}$ is the A_3 at very large wire diameter. Physical properties of the wires and the liquids at saturation temperature are given in Table 5.

Wire temperature

Figures 10a–10c show the wire temperature distribution calculated by Eq. 27. Figure 10a shows the effect of wire diameter when liquid and wire material are the same. The smaller the wire diameter, the shorter the L_E and the steeper the temperature profile. Figure 10b shows the effect of wire material when liquid and wire diameter are the same. Ti wire has smaller L_E and steeper temperature profile than the others. In fact, L_E of W wire is 3.75 times that of Ti wire, a result mainly due to thermal conductivity for which W is about 8.3 times that of Ti. This figure also shows that Mo wire behaves very much like W wire. Figure 10c shows that different liquids used in this work have negligible effect on temperature distribution.

Transition velocity

Figure 11 shows experimental transition velocity, u_{exp}, plot-

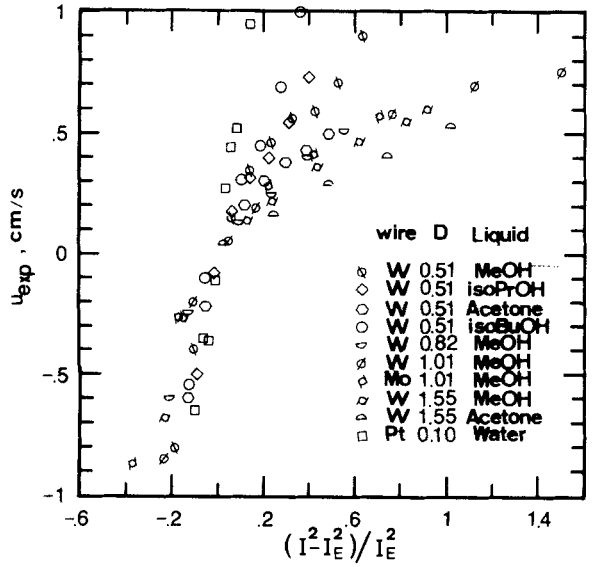

Figure 11. Experimental transition velocity vs. $(I^2-I_E^2)/I_E^2$.

ted against the relative input energy, $(I^2-I_E^2)/I_E^2$. The origin (0,0) represents the STMB. The positive velocity is for advancing film boiling and the negative velocity is for receding film boiling. Data in this figure show that the further away the UTMB from the STMB, the faster the transition velocity. At the same absolute value of the abscissa, the receding velocity appears to be greater than the advancing velocity. This is due to the concave upward shape of the film boiling curve which makes the change in the magnitudes of N_B associated with the change in I when $I>I_E$ to be greater than the change in N_B associated with the change in I when $I<I_E$. Also, as the region above the film boiling curve but below the STMB curve is much smaller than the open region above the STMB curve,

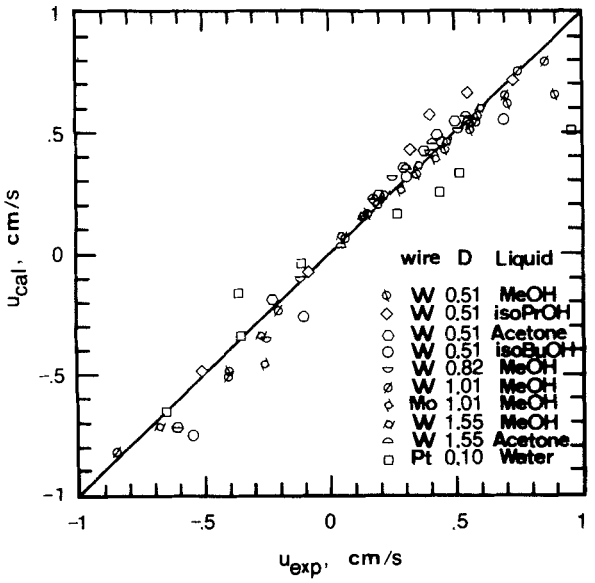

Figure 12. Comparison of experimental and calculated transition velocities.

□ Zhukov (1980).

experimental measurements are more difficult in the first region than in the second region. The data also show that at the same abscissa, transition zone on smaller wire travels faster. For Mo wire, the data points follow closely those for W wires of the same diameter. Some of the experimental data were not included in Figure 11. For example, for Ti wire, transition from α phase to β phase occurs at 880°C. For Ti wires 1.01 and 1.51 mm dia., I_E are 25.2 and 43.2 Amp respectively and T_F for both wires can reach 880°C. To avoid this temperature, Ti wires of smaller diameters may be considered. However, thermal expansion of Ti wires are significant and wires tend to be deformed. Transition velocity for Ti wires were therefore not included. It should be noted here that transition velocity on Ti wire is strikingly slow when compared with that for other wires. The velocity data of 0.15 mm W wire were also not included in Figure 11. This is because due to the fineness of the wire, the workable range of the applied currents becomes narrow (around 5 to 7 amperes). Outside of this current range, the wire is either too bright or too dark, and inside this current range, as the fluctuation of the output current from the DC generator amounts to about 0.4 Amp, velocity measurement for a given applied current becomes less dependable. The velocity data of Ta wire were not taken as Ta reacts with methanol at high temperature, and as swelling and melting of wire occur within the temperature range of investigation.

In Figure 12, transition velocity calculated by Eq. 40 is plotted against the experimentally measured transition velocity. The solid line represents the equation $y=x$. Figure 12 shows that the agreement between the calculation and experiment is good. Zhukov et al. (1980) measured transition velocity on a 0.1-mm Pt wire in saturation boiling of water at 98°C. Their experimental velocity data were compared with those calculated by Eq. 40. Data for the Pt-water system are also given in Tables 1 to 5. Figure 12 shows that good agreement is obtained. Zhukov et al. also proposed a velocity equation. However, they assumed constant heat-transfer coefficients in nucleate and film boiling regions. In view of their equation $\theta_{cr}=n/(1+n)$, their Eq. 5 should be $\alpha\sqrt{2/kD}[h_2\theta(1-\theta)^2-h_1\theta^2)]/\sqrt{h_2\theta(1-\theta)^2+h_1\theta^2(1-\theta)}$. This equation is an explicit equation and is numerically somewhat different from the exact solution we obtained. The latter is an implicit equation and is of the following form:

$$\frac{(1-\theta)}{\theta}=\frac{(\sqrt{B^2+4\gamma_1}+B)}{(\sqrt{B^2+4\gamma_2}-B)} \tag{48}$$

where

$$\theta\equiv\frac{(T_*-T_1)}{(T_2-T_1)},\quad B\equiv\frac{u\rho C_p}{k},\quad \gamma_i\equiv 4h_i/Dk. \tag{49a, b, c}$$

$i=1, 2$ for nucleate and film boiling.

Zhukov et al. did not specify the methods for the evaluation of h_1, h_2 and T_*, therefore, the results of calculations are dependent on the choices of these values. Also, the assumption of a step change between linear nucleate boiling curve and linear film boiling curve is not a desirable representation of

the actual situations. Their equation, as well as the exact solution that we derived, predicted zone velocities that show the correct tendency of increase with increasing applied current, however, the magnitudes of the velocities differed significantly from that calculated by Eq. 40.

Conclusions

Steady boiling curve diagrams each consisting of a steady nucleate boiling curve, a steady film boiling curve, and a steady TMB curve that bridges the first two curves have been presented for various boiling systems of different liquids and heating wires. The equilibrium current along the steady TMB curve can be calculated by Eq. 12 using only a limited number of data that are respectively along the nucleate and film boiling curves and that are in the regions sufficiently close the equilibrium point.

For UTMB, boiling mode transits from two mode to OMB automatically. The velocity of this transition on a wire can be calculated by Eq. 40. This velocity is zero when TMB is steady. The further away the TMB is from the steady one, the greater the transition velocity.

Both the calculated results of equilibrium currents and transition velocities agreed well with those measured by experiments.

Acknowledgment

The authors are grateful to the National Science Council, R. O. C. for supporting project NSC77-0402-E002-08.

Notation

A_C = cross-section area of the wire, m^2
A_3, A_2, A_1, A_0 = coefficients in Eq. 14
$A_{3,\infty}$ = constant (=0.00357)
a_2, a_1, a_0 = coefficients in Eq. 3
B = $u\rho C_p/k$ defined in Eq. 49b
b_4, b_3, b_2, b_1, b_0 = coefficients in Eq. 17
C = integration constant in Eq. 15
C_p = heat capacity of metal, J/kg·K
c_3, c_2, c_1, c_0 = coefficients defined in Table 3
D = diameter, m
$G(T_n, T_f)$ = function defined in N_G
g = gravitation acceleration, 9.8 m/s^2
h_1 = nucleate boiling heat-transfer coefficient, W/m^2·K
h_2 = film boiling heat-transfer coefficient, W/m^2-K
I = electric current, Amp
I_E = equilibrium current, Amp
i = dummy index
k = thermal conductivity, J/m·s·K
L = zone width with current I, m
L_E = zone width with equilibrium current, m
l = wire length, m
m, m' = defined in Eqs. 10 and 12
N_B = boiling loss group defined in Eq. 38b
N_G = generation group defined in Eq. 38a
$\overline{N}$ = number of Δq used in evaluating Eq. 12
N_3, N_2, N_1, N_0 = coefficients in Eq. 15a ~ 15d
n = $\sqrt{h_2/h_1}$
p, p^* = pressure, equilibrium pressure, $N\cdot m^{-2}$
$Q(T, I)$ = function defined in Eq. 2a
q = function defined in Eq. 2b
q_B = boiling heat flux, W/m^2
$\overline{q}_B$ = mean film boiling heat loss with current I, W/m^2
$\overline{q}_{B,E}$ = mean film boiling heat loss with current I_E, W/m^2
$q_{B,F}$ = equilibrium film boiling heat flux, W/m^2
$q_{B,N}$ = equilibrium nucleate boiling heat flux, W/m^2
q_f = film boiling heat flux, $w\cdot m^{-2}$
$\underline{T}$ = excess temperature, K
$\overline{T}$ = mean excess temperature defined in Eq. 34a, K
$\overline{\overline{T}}(T_1, T_2)$ = $1/2(T_1 + T_2) + T_{sat}$
$\overline{T}_E$ = mean excess temperature in STMB defined in Eq. 34b, K
T_E = excess temperature for STMB, K
T_F = excess temperature at point F, K
T_f = excess temperature at point f, K
T_N = excess temperature at point N, K
T_n = excess temperature at point n, K
T_{sat} = saturation temperature, K
T_0 = $(T_n + T_f)/2$, K
T_1 = nucleate boiling temperature, K
T_2 = film boiling temperature, K
T_* = Leidenfrost temperature, K
t = time, s
u = transition velocity, m/s
$V(T)$ = function defined in Eq. 19
v = volume, m^3
x = spatial coordinate, m
x_l, x_g = dv/dp, l in liquid phase, g in gas phase
z = $x - ut$, m

Greek letters

α = thermal diffusivity, m^2/s
β = parameter defined in Eq. 28
γ_i = $4h_i/Dk$
λ_c = critical wave length, m
ϕ = constant (=2.83) in Eq. 31
ρ = metal density, kg/m^3
ρ_l = liquid density, kg/m^3
ρ_v = vapor density, kg/m^3
ρ_T = resistivity at temperature T, Ohm·m
σ = surface tension, N/m
θ = $(T_* - T_1)/(T_2 - T_1)$
θ_{cr} = θ at zero velocity

Subscripts

F = intersection point of film boiling curve and equilibrium line
f = film boiling
g = gas
l = liquid
N = intersection point of nucleate boiling curve and equilibrium line
n = nucleate boiling
v = vapor

Literature Cited

Breen, B. P., and J. W. Westwater, "Effect of the Diameter of Horizontal Tubes on Film Boiling Heat Transfer," *Chem. Eng. Prog. Symp. Ser.*, **58**, 67 (1962).

Cubbery, W. H., and H. Baker, ed., *Metals Handbook*, v2, *Properties and Selection Nonferrous Alloy and Pure Metals*, 9th ed., ASM Handbook Committee (1979).

Fedorov, V. I., and N. P. Timchenko, "Determination of the Rate of Travel of Boiling Modes (Zones) on Nonisothermal Surfaces," *Heat Transfer—Soviet Research*, **15**, 37 (1983).

Hahne, E., and U. Grigull, *Heat Transfer in Boiling*, p. 162, Eq. 3, Academic Press, NY (1977).

Hampel, C. A., ed., *Rare Metals Handbook* (1961).

Lin, K. S., "Pressure Effect on Boiling Heat Transfer," MS Thesis, National Taiwan University, Chem. Eng. Dept., Taiwan (July, 1986).

Lu, S. M., and D. J. Lee, "The Effects of Heating Methods on Pool

Boiling," *Int. J. Heat Mass Transfer*, **34**(1), 127 (1991).
Pippard, A. B., "Response and Stability, An Introduction to the Physical Theory," Cambridge Univ. Press (1985).
Semeria, R., and B. Martinet, "Calefaction Spots on a Heating Wall: Temperature Distribution and Resorption," *Symp. on Boiling Heat Transfer in Steam Generating Units and Heat Exchangers*, p. 192, Manchester (1965).
Smithells, C. J., and E. A. Brandes, *Metals Reference Book*, 5th ed., Butterworths (1976).
Timchenko, N. P., S. A. Zhukov, K. G. Shkadinskiy, and V. I. Fedorov, "Effect of the Shape of the Boiling Curve on the Dynamics of Self-Generated Waves," *Heat Transfer—Sov. Res.*, **16**, 67 (1984)
Van Ouwerkerk, H. J., "Burnout in Pool Boiling the Stability of Boiling Mechanisms," *Int. J. Heat Mass Transfer*, **15**, 25 (1972).
Weber, G., "Abrupt transitions in Physics and Biophysics: van der Walls Revisited," *Proc. Nat. Acad. Sci.*, **84**, 7359 (1987).
Yamanouchi, A., "Effect of Core Spray Cooling in Transient State after Loss of Coolant Accident," *J. Nucl. Sci. and Technol.*, **5**, 547 (1968).
Zhukov, S. A., V. V. Barelko, and A. G. Merzhanov, "Wave Processes on Heat Generating Surfaces in Pool Boiling," *Int. J. Heat Mass Transfer*, **24**, 47 (1980).
Zhukov, S. A., and V. V. Barelko, "Nonuniform Steady States of the Boiling Process in the Transition Region between the Nucleate and Film Regimes," *Int. J. Heat Mass Transfer*, **26**, 1130 (1983).
Zhukov, S. A., L. F. Bokova, and V. V. Barelko, "Certain Aspects of Autowave Transitions from Nucleate to Film Boiling Regimes with a Cylindrical Heat Generating Element Inclined from a Horizontal Position," *Int. J. Heat Mass Transfer*, **26**, 269 (1983).

Manuscript received June 10, 1991, and revision received April 20, 1992.